Chemical Engineering Science, Vol. 44, No. 12, pp. 2809–2816, 1989.
Printed in Great Britain.

0009-2509/89 $3.00 + 0.00

NUMERICAL SIMULATION OF A PRESSURE SWING ADSORPTION OXYGEN UNIT

S. FAROOQ, D. M. RUTHVEN† and H. A. BONIFACE‡
Department of Chemical Engineering, University of New Brunswick, Fredericton, N.B., Canada E3B 5A3

(*Received* 9 *August* 1988; *accepted for publication* 17 *April* 1989)

Abstract—The numerical model, originally developed to simulate the kinetic separation of air in a carbon molecular sieve pressure swing adsorption unit, has been extended and applied to the equilibrium selective separation of air over a zeolite adsorbent in which nitrogen is preferentially adsorbed, leaving oxygen as the (pure) raffinate product. The model, which assumes binary Langmuir equilibrium with linearized mass transfer rate expressions, is shown to provide a good representation of the performance of a small experimental unit over a range of operating conditions.

INTRODUCTION

In previous publications (Hassan *et al.*, 1986, 1987) we have discussed the modelling and simulation of pressure swing adsorption (PSA) units for nitrogen production. These units use a carbon molecular sieve adsorbent which is kinetically selective for oxygen. Oxygen is the faster diffusing species and is preferentially adsorbed even though, at equilibrium, the affinities for oxygen and nitrogen are almost the same. For oxygen production it is preferable to use a nitrogen-selective adsorbent, the common choice being 5A zeolite which, at ambient temperature, exhibits an equilibrium separation factor of about 3.0 in favour of nitrogen.

The simplest approach to the modelling of an equilibrium-controlled PSA separation process involves the use of equilibrium theory (Knaebel and Hill, 1985; Kayser and Knaebel, 1986, 1989). The advantage of this approach is that it allows analytic solution of the governing material balance equations by the method of characteristics. The approach is, however, limited to the idealized case where there are no dispersive effects such as axial mixing or finite resistance to mass transfer. (Under these conditions a perfectly pure raffinate product is obtained.) Equilibrium theory does not allow easy extension to the real situation where dispersive effects are significant and product purity is limited. Furthermore, in real PSA systems there are two problems with this approach. In bulk separations where the velocity varies through the bed the characteristic lines are curved and, although an analytic solution for the concentration front may still be obtained, except in the case of a linear isotherm, the solution will be in the form of a cumbersome integral which requires numerical evaluation (Kayser and Knaebel, 1989). A more serious difficulty arises in tracking the concentration waves for adsorption and desorption in partially loaded beds since, depending on the initial profile and the form of the equilibrium relationship, one may observe the formation of combined wave fronts (e.g. partial shock plus simple wave). Under these conditions the simple model breaks down and it is necessary to track both waves and the transition point simultaneously (Flores-Fernandez and Kenney, 1983).

The equilibrium theory solution will provide preliminary design guidance and useful insight into the system behaviour. However, a more realistic model including axial dispersion and mass transfer resistance is necessary for detailed optimization studies. We have therefore adapted the linear driving force (LDF) dynamic model originally developed by Hassan *et al.* (1986, 1987) for a nitrogen PSA system. The major modifications required concern the pressurization and blowdown steps. In the kinetically controlled nitrogen PSA simulation we assume that the adsorbed-phase concentrations remain frozen during these steps since mass transfer is relatively slow. While this is an acceptable approximation for a kinetically controlled system where mass transfer rates are relatively slow, it is clearly inappropriate for an equilibrium-controlled process where the mass transfer rates may be very much higher. For the present application the model was therefore modified to include the full solution of the mass transfer equations during pressurization and blowdown steps. The model predictions, using independently determined parameters, are shown to provide a good representation of the performance of a small laboratory scale PSA oxygen unit with 5A zeolite as the adsorbent.

A pore diffusion model for bulk separation of a binary mixture was developed by Yang and Doong (1985) and shown to provide a reasonably good representation of the separation of a 50–50 mixture of H_2–CH_4 on activated carbon, and one may assume that the same scheme could be adapted to the case of air separation on a zeolite. However, in an equilibrium-controlled process the detailed form of the kinetic model is of only secondary importance. There therefore appears to be very little advantage to be gained from using the pore diffusion model rather than the simpler and computationally quicker LDF model. Moreover, although Yang and Doong (1985)

†Author to whom correspondence should be addressed.
‡Presently with Atomic Energy of Canada Ltd., Chalk River, Ontario, Canada.

have formulated their problem in terms of the pore diffusion model, they actually solve the model equations with the aid of the simplifying assumption that the intraparticle concentration profile is parabolic. The parabolic concentration profile approximation corresponds to a fully developed concentration profile in a particle which requires a large cycle time and/or rapid mass transfer. The pore model solution of Yang and Doong will therefore prove inadequate when the cycles are short. Direct support for this argument is obtained from the recent work of Do and Mayfield (1987). For the LDF model approach, available correlations (Raghavan *et al.*, 1986) allow adjustment of the model constant for any cycle time. Thus the LDF model approach taken in the present study not only reduces the computational complexity but will also be applicable to those situations in which the assumption of a parabolic concentration profile in an adsorbent particle breaks down.

THEORETICAL MODEL

A simple two-bed process operated on a Skarstrom cycle is considered, as shown in Fig. 1. The following four steps comprise the cycle:

(1) pressurization,
(2) adsorption,
(3) countercurrent blowdown,
(4) countercurrent purge.

In step 1, bed 2 is pressurized to the high operating pressure with feed from the feed end and bed 1 is blown down to the atmospheric pressure in the reverse flow direction. In step 2, the high-pressure feed flows through bed 2. The more strongly adsorbed component is retained in the bed and a gas stream enriched in the lighter component leaves as effluent. A fraction of the effluent stream is withdrawn as product and the rest is used for countercurrent purge of bed 1 at a reduced pressure. The operations are switched between the beds in steps 3 and 4. In order to develop a mathematical model for this system the following assumptions are introduced:

(1) The system is assumed to be isothermal. In a large-scale system this would probably not be a good approximation. However, in the present study small-diameter thick walled metal columns were used and the high heat capacity and thermal conductivity of the column walls serve to minimize temperature variations.
(2) The frictional pressure drop in the bed is negligible.
(3) The total pressure in the bed remains constant during the adsorption and purge steps (steps 2 and 4).
(4) During pressurization and blowdown the total pressure in the bed changes linearly with time.
(5) The fluid velocity in the bed varies along the length of the column, as determined by the overall mass balance.
(6) The flow pattern is described by the axial dispersed plug flow model. In a collocation system use of the dispersed plug flow model, even with a relatively high Peclet number, facilitates the computation by slightly rounding the concentration profiles.
(7) Equilibrium relationships for both components are represented by binary Langmuir isotherms.
(8) The mass transfer rates are represented by linear driving force rate expressions in which the coefficients are taken to be pressure-dependent. While a pore diffusion model may be more realistic it is computationally much more time-consuming and, in an equilibrium-dominated system, can be expected to lead to only minor differences in the calculated profiles. We therefore use the simpler LDF form.
(9) The ideal-gas law applies.
(10) The presence of argon, which is adsorbed with almost the same affinity as oxygen and therefore appears with oxygen in the raffinate product, is ignored.

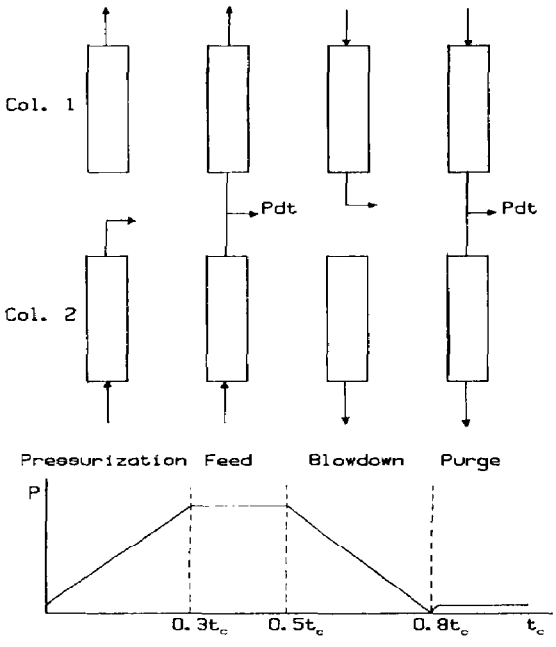

Fig. 1. Schematic diagram of the PSA cycle.

Subject to these assumptions, the system of equations describing the cyclic operation is as follows:

Step 1: pressurization of bed 2 and blowdown of bed 1
Material balance for bed 2 (component A):

$$-D_L\frac{\partial^2 c_{A2}}{\partial z^2}+v_2\frac{\partial c_{A2}}{\partial z}+c_{A2}\frac{\partial v_2}{\partial z}+\frac{\partial c_{A2}}{\partial t}+\frac{1-\varepsilon}{\varepsilon}\cdot\frac{\partial q_{A2}}{\partial t}=0 \quad (1)$$

Continuity condition:

$$c_{A2}+c_{B2}=C_2\neq f(z)=f(t) \tag{2}$$

Overall material balance:

$$C_2\frac{\partial v_2}{\partial z}+\frac{\partial C_2}{\partial t}+\frac{1-\varepsilon}{\varepsilon}\left(\frac{\partial q_{A2}}{\partial t}+\frac{\partial q_{B2}}{\partial t}\right)=0 \tag{3}$$

Mass transfer rates:

$$\frac{\partial q_{A2}}{\partial t}=k_{A2}(q^*_{A2}-q_{A2}),\quad \frac{\partial q_{B2}}{\partial t}=k_{B2}(q^*_{B2}-q_{B2}) \tag{4}$$

Adsorption equilibrium:

$$\frac{q^*_{A2}}{q_{AS}}=\frac{b_Ac_{A2}}{1+b_Ac_{A2}+b_Bc_{B2}},\quad \frac{q^*_{B2}}{q_{BS}}=\frac{b_Bc_{B2}}{1+b_Ac_{A2}+b_Bc_{B2}} \tag{5}$$

Boundary conditions:

$$D_L\frac{\partial c_{A2}}{\partial z}\bigg|_{z=0}=-v_o(c_{A2}|_{z=0^-}-c_{A2}|_{z=0}),\quad \frac{\partial c_{A2}}{\partial z}\bigg|_{z=L}=0. \tag{6}$$

Note that in a commercial operation the feed stream would be supplied by compressors. Hence a constant-flow situation is probably more appropriate rather than a constant-pressure feed stream. Therefore, during pressurization the inlet velocity v_o changes with changing column pressure.

Material balance for bed 1 (component A):

$$-D_L\frac{\partial^2 c_{A1}}{\partial z^2}+v_1\frac{\partial c_{A1}}{\partial z}+c_{A1}\frac{\partial v_1}{\partial z}+\frac{\partial c_{A1}}{\partial t}+\frac{1-\varepsilon}{\varepsilon}\cdot\frac{\partial q_{A1}}{\partial t}=0 \tag{7}$$

Continuity condition:

$$c_{A1}+c_{B1}=C_1\neq f(z)=f(t) \tag{8}$$

Overall material balance:

$$C_1\frac{\partial v_1}{\partial z}+\frac{\partial C_1}{\partial t}+\frac{1-\varepsilon}{\varepsilon}\left(\frac{\partial q_{A1}}{\partial t}+\frac{\partial q_{B1}}{\partial t}\right)=0 \tag{9}$$

Mass transfer rates:

$$\frac{\partial q_{A1}}{\partial t}=k_{A1}(q^*_{A1}-q_{A1}),\quad \frac{\partial q_{B1}}{\partial t}=k_{B1}(q^*_{B1}-q_{B1}) \tag{10}$$

Adsorption equilibrium:

$$\frac{q^*_{A1}}{q_{AS}}=\frac{b_Ac_{A1}}{1+b_Ac_{A1}+b_Bc_{B1}},\quad \frac{q^*_{B1}}{q_{BS}}=\frac{b_Bc_{B1}}{1+b_Ac_{A1}+b_Bc_{B1}} \tag{11}$$

Boundary conditions:

$$\frac{\partial c_{A1}}{\partial z}\bigg|_{z=0}=0,\quad \frac{\partial c_{A1}}{\partial z}\bigg|_{z=L}=0. \tag{12}$$

Equation (6), which defines the standard (Dankwerts) inlet and exit boundary conditions for a dispersed plug flow system, reduces to eq. (12) when the inlet velocity is set to zero.

Step 2: high-pressure adsorption in bed 2 and purge in bed 1

For bed 2 other than the following changes all the equations for step 1 remain unchanged in step 2.

Continuity condition:

$$c_{A2}+c_{B2}=C_H\ \text{(constant)} \tag{13}$$

Overall material balance:

$$C_H\frac{\partial v_2}{\partial z}+\frac{1-\varepsilon}{\varepsilon}\left(\frac{\partial q_{A2}}{\partial t}+\frac{\partial q_{B2}}{\partial t}\right) \tag{14}$$

Boundary condition at the inlet:

$$D_L\frac{\partial c_{A2}}{\partial z}\bigg|_{z=0}=-v_{OH}(c_{A2}|_{z=0^-}-c_{A2}|_{z=0}). \tag{15}$$

Similarly for bed 1, except for the following changes, all the equations in step 1 remain unchanged in step 2:

Continuity condition:

$$c_{A1}+c_{B1}=C_L\ \text{(constant)} \tag{16}$$

overall material balance:

$$C_L\frac{\partial v_1}{\partial z}+\frac{1-\varepsilon}{\varepsilon}\left(\frac{\partial q_{A1}}{\partial t}+\frac{\partial q_{B1}}{\partial t}\right) \tag{17}$$

Boundary condition at the inlet:

$$D_L\frac{\partial c_{A1}}{\partial z}\bigg|_{z=0}=-v_{OL}(c_{A1}|_{z=0^-}-c_{A1}|=_{z=0}) \tag{18}$$

$$c_{A1}|_{z=0^-}=\left(\frac{P_L}{P_H}\right)c_{A2}|_{z=L}. \tag{19}$$

The equations describing the operations in the two beds in steps 1 and 2 are interchanged in steps 3 and 4, but with the change in the direction of flow taken into account.

The appropriate initial conditions for the start-up of the cyclic operation from a clean bed are as follows:

$$\begin{aligned} &c_{A2}(z,0)=0;\quad c_{B2}(z,0)=0\\ &q_{A2}(z,0)=0;\quad q_{B2}(z,0)=0\\ &c_{A1}(z,0)=0;\quad c_{B1}(z,0)=0\\ &q_{A1}(z,0)=0;\quad q_{B1}(z,0)=0. \end{aligned} \tag{20}$$

Equations (1)–(20) were rearranged and written in the dimensionless form. The dimensionless equations were then solved by the method of orthogonal collocation to give gas and solid phase concentrations of oxygen and nitrogen as a function of the dimensionless bed length (z/L) for various values of time. Five internal collocation points were used. Details of the collocation form are given elsewhere (Farooq, 1988). Computations were continued until a cyclic steady state was achieved. Depending on the parameter values 15–25 cycles were required to attain the cyclic steady state.

EXPERIMENTAL

The experimental studies were carried out on the same small laboratory scale two-bed PSA unit as used in our earlier studies of nitrogen production (Hassan *et al.*, 1986), except that the carbon adsorbent was replaced by a 5A zeolite molecular sieve. The oxygen

concentration in the raffinate product was monitored continuously using a Servomex OA 137 paramagnetic oxygen analyser, and the sequence of valve switching was controlled by a Xanadu universal programmable timer. The flow rates of the feed air and product oxygen were controlled by Matheson flow controllers, and the outputs from the flow meters and oxygen analyzer were monitored continuously on a multiple-channel strip chart recorder. Prior to experimental studies the adsorbent beds were regenerated at 420°C for 12 h under a helium purge in order to eliminate moisture from the adsorbent.

The system was operated at several different feed and product withdrawal rates, and at different pressures. In general between 20 and 30 full cycles were required to approach the cyclic steady state. The transient behaviour was followed only in order to determine that the steady state had been reached and, in the numerical simulations, we have therefore focused entirely on the prediction of the steady-state operation; no attempt has been made to analyse the transient.

ESTIMATION OF PARAMETER VALUES

The equilibrium and kinetic parameters used in simulating the experimental runs are summarized in Table 1, together with details of the adsorbent, the bed dimensions and the cycle.

The effective LDF rate constants for oxygen and nitrogen have been calculated from the following expression:

$$k = \Omega \frac{\varepsilon_p D_p}{R_p^2}\left(\frac{c_o}{q_o}\right) \tag{21}$$

Table 1. Kinetic and equilibrium data and other common parameter values used in the simulations

Feed composition	21% oxygen, 79% nitrogen
Adsorbent	Linde 5A zeolite
L (cm)	35.0
r_i (cm)	1.75
d_p (cm)	0.0707
ε	0.40
T_o (°C)	25.0
Blowdown pressure (atm)	1.0
Purge pressure (atm)	1.07 ± 0.05
Peclet number	500.0
Duration of step 1 or 3	0.3 of total cycle time
Duration of step 2 or 4	0.2 of total cycle time
Equilibrium constant for oxygen (K_A)	4.7†
Equilibrium constant for nitrogen (K_B)	14.8†
LDF constant for oxygen (k_A) (s^{-1})	62.0 (at 1 atm)
LDF constant for nitrogen (k_B) (s^{-1})	19.7 (at 1 atm)
Saturation constant for oxygen (q_{AS}) (mol/cm^3)	5.26×10^{-3}‡
Saturation constant for nitrogen (q_{BS}) (mol/cm^3)	5.26×10^{-3}

†Chromatographic data (Boniface, 1983).
‡Miller *et al.* (1987).

which assumes macropore diffusion control. The diffusion of oxygen and nitrogen in 5A zeolite has been studied chromotographically by Haq and Ruthven (1986). Their results showed that, even in the relatively small particles used in this study, macropore resistance is more important than micropore resistance, although the major dispersive effect was axial dispersion. In the present study, since the pressure is always greater than atmospheric, we have neglected any contribution from Knudsen diffusion and estimated the macropore diffusivity assuming molecular diffusion control with a tortuosity factor of 3.0 and a particle porosity of 0.33.

The factor Ω depends on the dimensionless cycle time according to the correlation established by Raghavan *et al.* (1986). However, the experimental conditions covered by the present study all lie within the large cycle time region for which Ω approaches the Glueckauf limit of 15. The value of Ω for both oxygen and nitrogen was therefore set at 15 throughout.

The pressure dependence of the LDF rate constant for the case of molecular diffusion control has been given by Hassan *et al.* (1985):

$$\frac{k_2}{k_1} = \frac{1}{\left(\frac{P_H}{P_L}\right) - \lambda_{HP}\left[\left(\frac{P_H}{P_L}\right) - 1\right]}.$$

The curvature of the oxygen and nitrogen isotherms on 5A zeolite is modest, and neglecting the second term in the denominator on the right-hand side of the above equation did not affect the simulation. Therefore, the LDF rate constants for oxygen and nitrogen were taken as inversely proportional to pressure.

The saturation capacity for oxygen (q_{AS}) has been taken for the recent work of Miller *et al.* (1987). Since oxygen and nitrogen molecules are about the same size their saturation capacities were assumed to be the same. The Henry constants for oxygen and nitrogen were determined experimentally from the first moments of their chromatographic response (Boniface, 1983).

Peclet numbers (based on interstitial inlet velocity during the high-pressure step) calculated from the correlation of Hsu and Haynes (1981) are in the range of 200–225, whereas the values predicted by the correlation of Edwards and Richardson (1968) are in the range 700 800. The simulation was run under a representative set of operating conditions with Peclet numbers in the range 200–700 and the results showed very little effect on the purity or recovery of the oxygen product. A constant value of 500 was therefore used for all four steps.

RESULTS AND DISCUSSION

The experimentally observed product purity and recovery for several operating conditions are summarized in Table 2, together with the theoretically predicted values from the numerical simulation. The mole percent of oxygen in the product refers to the average oxygen concentration in the product at steady

Table 2. Summary of experimental conditions, product purity and recovery

Experiment No.	Feed flow rate† (cm^3/s)	Product flow rate† (cm^3/s)	Cycle time (s)	Adsorption pressure (atm)	Mole % O_2 in product		Recovery of O_2 (%)	
					Experiment	Theory	Experiment	Theory
1	25.0	1.13	100	1.48	80.0	93.4 92.6‡	17.0	20.1 19.9‡
2	25.0	1.13	150	1.66	92.0	96.4 96.2‡	19.9	20.8 20.7‡
3	25.0	1.13	200	1.73	86.0	78.2 74.8‡	18.5	16.8 16.1‡
4	25.0	1.13	250	1.90	72.0	76.7	15.5	16.5
5	33.3	1.13	200	2.33	95.5	94.7	15.4	15.3
6	50.0	1.13	200	3.41	91.0	95.8	9.8	10.3
7	66.7	1.13	160	4.30	95.5	96.3	7.7	7.8
8	66.7	2.55	160	4.35	95.3	96.4	17.4	17.6
9	66.7	3.98	160	4.26	95.5	96.2	27.1	27.3

†1 atm, 25°C.
‡Instant pressure change assumed during blowdown. All other theoretical results correspond to linear pressure change during blowdown.

state. The theoretical oxygen concentration in the product at steady state was therefore computed at short time intervals and was integrated to find the average. Since the product rate rather than the purge rate was fixed the recovery calculation was straight forward.

The effects of cycle time, adsorption pressure, and product withdrawal rate on the purity and recovery are shown in Figs 2–4. The effect of varying the blowdown conditions was also briefly investigated and the results are shown in Fig. 2. There is clearly very little difference between the simulation results for an instantaneous pressure change or a linear pressure change during blowdown.

Under properly selected conditions an oxygen product purity of greater than 95% was obtained. Under these conditions almost all the nitrogen is separated and the impurity in the oxygen is mainly the residual argon which is not separated. It is evident that the theoretical model gives a reasonably accurate prediction of both the purity and recovery of the oxygen product over the range of experimental variables examined. Perhaps, more importantly, the trends of purity and recovery with cycle time, adsorption pressure and product rate are correctly predicted. The model should therefore prove useful for optimization of the process cycle and for guidance in the choice of operating conditions for existing systems.

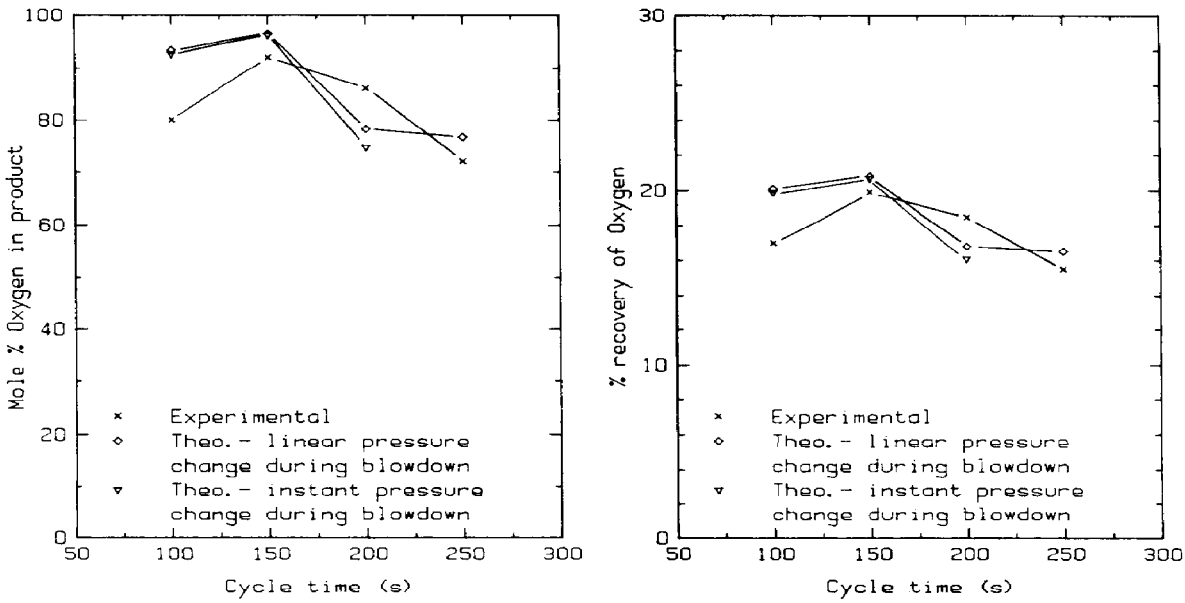

Fig. 2. Effect of cycle time on product purity and recovery. Operating parameters as for experiments 1–4 in Table 2; other parameters are given in Table 1.

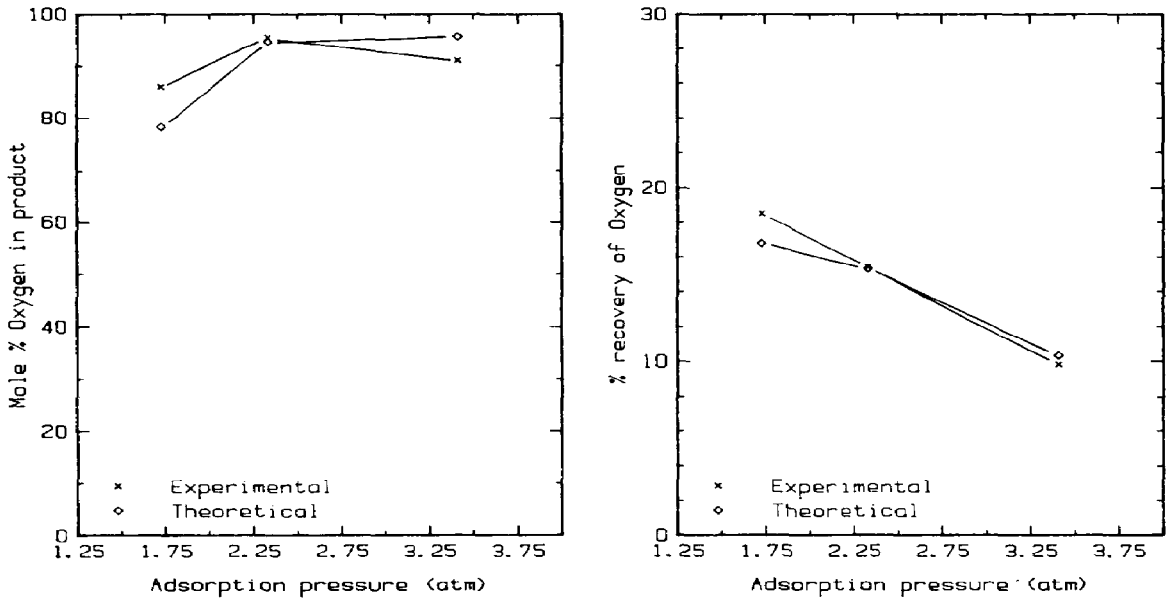

Fig. 3. Effect of adsorption pressure on product purity and recovery: experiments 3, 5 and 6 in Table 2. Other parameters are given in Table 1.

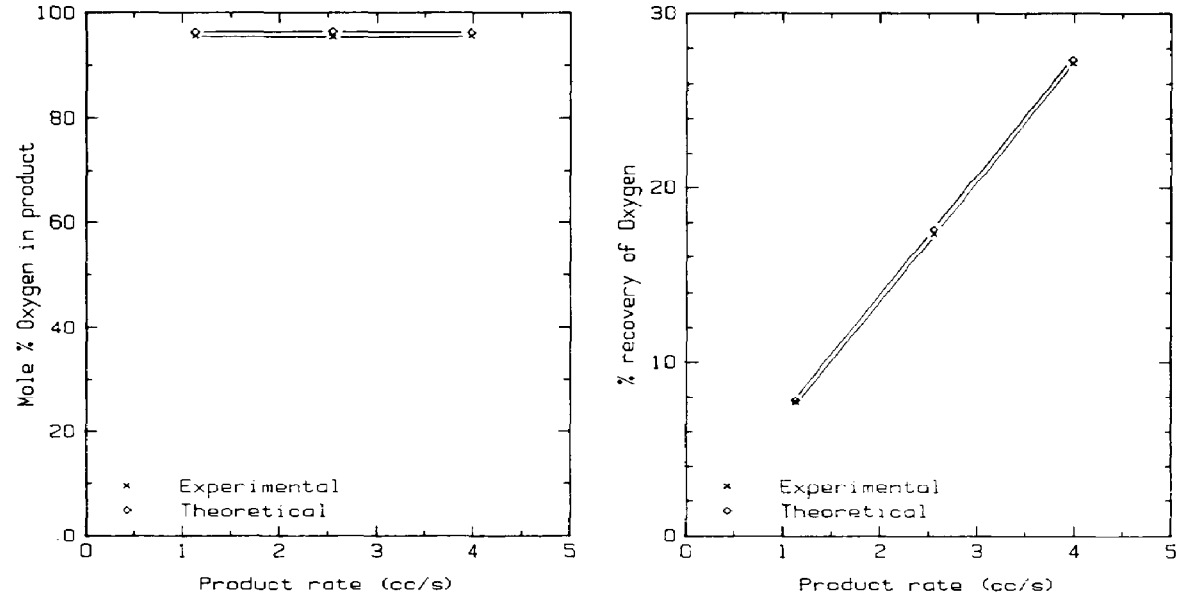

Fig. 4. Effects of product rate on product purity and recovery. Experimental conditions are given in Table 2 (experiments 7–9); other parameters are given in Table 1.

For two sets of operating conditions, represented by experiments 1 and 4 (Table 2), the effect on performance of varying the mass transfer resistance was investigated theoretically. The results are summarized in Table 3. Under the conditions of experiment 1 a high-purity product is obtained, showing that the system must be operating without significant breakthrough. Reducing the mass transfer coefficients by a factor of 3 (case 2 of Table 3) gave very little change in either the purity or recovery of the oxygen product, implying that under these conditions the system is operating close to equilibrium. Under the conditions of experiment 4 (Table 2) the effect of increasing the mass transfer resistance is more pronounced (cases 3 and 4 of Table 3) since under these conditions there is significant breakthrough and any broadening of the concentration front as a result of increased mass transfer resistance leads to a lower-purity product.

Table 3. Effect of mass transfer resistance on product purity and recovery†

No.	Feed rate (cm^3/s)	Product rate (cm^3/s)	k_A (s^{-1})	k_B (s^{-1})	Mole % O_2 in product	Recovery of O_2 (%)
1	25.0	1.13	62.0	19.7	93.40	20.10
2	25.0	1.13	20.0	6.6	93.29	20.08
3	25.0	1.13	62.0	19.7	76.70	16.50
4	25.0	1.13	20.0	6.6	75.78	16.30

† For 1 and 2: adsorption pressure = 1.48 atm, blowdown pressure = 1.0 atm, purge pressure = 1.07 atm, cycle time = 100 s; for 3 and 4: adsorption pressure = 1.90 atm, blowdown pressure = 1.0 atm, purge pressure = 1.1 atm, cycle time = 250 s. Other parameters as in Table 1.

Figure 4 shows that, under the conditions of experiments 7–9, oxygen recovery increases continuously with increasing product rate and there is very little change in product purity. Presumably at higher product withdrawal rates the purity will eventually decline.

The effect of purge rate on the purity and recovery of oxygen was investigated theoretically. For other operating conditions similar to experiment 7 (Table 2) it was found that the recovery decreases with increasing purge rate as expected. The purity initially increases and then becomes almost constant at higher purge rates (purge to feed velocity ratio > 1.5).

In the situation where the feed volume, rather than the pressure, is kept constant it will be more appropriate to use the actual pressure–time history of the bed during pressurization rather than making the linear approximation. The pressure–time history of the bed during pressurization, if available, can be easily incorporated in the existing computer code.

The present model assumes that the pressure within the bed remains constant during the adsorption step. In an actual operation the column pressure will continue to increase during the adsorption step. This is not an operational constraint, rather the changing pressure during the adsorption step can be exploited to improve the system performance (Kayser and Knaebel, 1989). Extension of the present model to handle pressure changes during the adsorption step would be straightforward.

CONCLUSIONS

The dynamic simulation previously developed for a kinetically controlled nitrogen PSA system has been successfully modified and applied to an oxygen PSA cycle, in which the equilibrium, rather than kinetic effect, is dominant. The advantage of this approach over the equilibrium theory approach which has been applied previously to this type of system is that it allows easy investigation of the effects of mass transfer resistance and axial dispersion on system performance. The cycle used here is the simple two-bed Skarstrom cycle but there is no reason to prevent the application of the same model to the more complex multibed systems which are commonly used in larger-scale units.

NOTATION

b_A, b_B Langmuir constant for component A, for component B

c_{A1}, c_{A2} concentration of component A in gas phase in bed 1, in bed 2

c_{B1}, c_{B2} concentration of component B in gas phase in bed 1, in bed 2

c_o sorbate concentration in feed gas

C_H, C_L, C_1, C_2 total gas phase concentration at high pressure, at purge pressure, during blowdown, during pressurization

d_p particle diameter

D_L axial dispersion coefficient

D_p macropore diffusivity

k_A (k_{A1}, k_{A2}) effective mass transfer coefficient for component A (in bed 1, in bed 2)

k_B (k_{B1}, k_{B2}) effective mass transfer coefficient for component B (in bed 1, in bed 2)

K_A, K_B adsorption equilibrium constant for oxygen at T_o, for nitrogen at T_o

L bed length

P (P_H, P_L) column pressure (for high-pressure step, for low-pressure step)

q_{A1}, q_{A2} concentration of component A in solid phase in bed 1, in bed 2

q_{B1}, q_{B2} concentration of component B in solid phase in bed 1, in bed 2

q_S (q_{AS}, q_{BS}) saturation constant (for component A, for component B)

q_o concentration in solid phase in equilibrium with c_o

q^*_{A1}, q^*_{A2} value of q_{A1} in equilibrium with c_{A1}, of q_{A2} in equilibrium with c_{A2}

q^*_{B1}, q^*_{B2} value of q_{B1} in equilibrium with c_{B1}, of q_{B2} in equilibrium with c_{B2}

r_i inner radius of column

R_p particle radius

t (t_c) time (cycle time)

T_o ambient temperature

v_2, v_1 interstitial velocity in bed 2, in bed 1

v_o interstitial inlet velocity during pressurization

v_{OH} interstitial inlet velocity during high-pressure flow
v_{OL} interstitial inlet velocity during purge flow
z axial distance from column inlet
$0, (0^-)$ position just inside (just outside) column

Greek letters

ε bed voidage
ε_p particle voidage
λ_{HP} nonlinearity parameter at high pressure (q_o/q_s)
Ω constant in LDF rate expression

REFERENCES

Atomic Energy of Canada, 1976, A Fortran package for the automated solution of coupled and/or ordinary differential equation systems.

Boniface, H., 1983, Separation of argon from air using zeolites. Ph.D. thesis, University of New Brunswick, Fredericton.

Do, D. D. and Mayfield, P. L. J., 1987, A new simplified model for adsorption in a single particle. *A.I.Ch.E. J.* **33**, 1397–1400.

Edwards, M. F. and Richardson, J. F., 1968, Gas dispersion in packed beds. *Chem. Engng Sci.* **23**, 109–123.

Farooq, S., 1988, A study of pressure swing adsorption systems. Ph.D. thesis, University of New Brunswick, Freidericton.

Flores-Fernandez, G. and Kenney, C. N., 1983, Modelling of the pressure swing air separation process. *Chem. Engng Sci.* **38**, 827–834.

Haq, N. and Ruthven, D.M., 1986, A chromatographic study of sorption and diffusion in 5A zeolite. *J. Colloid Interface Sci.* **112**, 164–169.

Hassan, M. M., Raghavan, N. S., Ruthven, D. M. and Boniface, H. A., 1985, Pressure swing absorption—II. *A.I.Ch.E. J.* **31**, 2008–2016.

Hassan, M. M., Raghavan, N. S. and Ruthven, D. M., 1986, Air separation by pressure swing adsorption on a carbon molecular sieve. *Chem. Engng Sci.* **41**, 1333–1343.

Hassan, M. M., Raghavan, N. S. and Ruthven, D. M., 1987, Pressure swing adsorption air separation on a carbon molecular sieve—II. *Chem. Engng Sci.* **42**, 2037–2043.

Hsu, L. K. P. and Haynes, H. W., 1981, Effective diffusivity by the gas chromatography technique: analysis and application to measurements of diffusion of various hydrocarbons in zeolite NaY. *A.I.Ch.E. J.* **27**, 81–91.

Kayser, J. C. and Knaebel, K. S., 1986, Pressure swing adsorption: experimental study of an equilibrium theory. *Chem. Engng Sci.* **41**, 2931–2938.

Kayser, J. C. and Knaebel, K. S., 1989, Pressure swing adsorption: development of an equilibrium theory for binary gas mixtures with nonlinear isotherms. *Chem. Engng Sci.* **44**, 1–8.

Knaebel, K. S. and Hill, F. B., 1985, Pressure swing adsorption: development of equilibrium theory for gas separations. *Chem. Engng Sci.* **40**, 2351–2360.

Miller, G. W., Knaebel, K. S. and Ikels, K. G., 1987, Equilibria of nitrogen, oxygen, argon, and air in molecular sieve 5A. *A.I.Ch.E. J.* **33**, 194–201.

Raghavan, N. S., Hassan, M. M. and Ruthven, D. M., 1986, Numerical simulation of a PSA system using a pore diffusion model. *Chem. Engng Sci.* **41**, 2787–2793.

Yang, R. T. and Doong, S. J., 1985, Gas separation by pressure swing adsorption: a pore diffusion model for bulk separation. *A.I.Ch.E. J.* **31**, 1829–1842.